Optomechanical Properties of the Morphology of Viscose Fibers Due to the Cold-Drawing Process

I. M. Fouda, E. A. Seisa

Physics Department, Faculty of Science, Mansoura University, Mansoura, Egypt

Received 4 August 2007; accepted 15 April 2008
DOI 10.1002/app.28549
Published online 10 July 2008 in Wiley InterScience (www.interscience.wiley.com).

ABSTRACT: This study sheds light on the changes produced by the effects of cold-drawn fibers on the microstructure and macrostructure of viscose fibers. The optical properties and strain produced in viscose fibers were measured interferometrically at room temperature. Structural parameters were calculated, such as the work per unit of volume, the reduction in entropy due to elongation, and the harmonic mean specific refractivity. In addition, the resulting data were used to calculate the optical stress coefficient and optical configuration and to apply the Mooney–Rivlin equation to determine the constants. Also, the number of crystals per unit of volume and the average orientation angle for uniaxial stretching were calculated with the extension ratios. The relation between the true stress and strain hardening was calculated. The average value of the maximum birefringence was determined to equal 0.046. The relations between the optical and mechanical changes with different parameters were established for the studied fibers. Microinterferograms and curves were drawn for illustration.
 J Appl Polym Sci 110: 872–879, 2008

Key words: density; drawing; mechanical properties

INTRODUCTION

Natural, synthetic, and manmade fibers play important roles in the textile industry, in which most fibers are now mixed with others. Thus, an investigation of the characteristic properties of these fibers is important. Many studies have been conducted on the characterization of the structural, optical, and mechanical properties of viscose fibers.[1–5]

The application of the various interferometric methods to investigating the optical behavior of optically anisotropic fibrous materials has been discussed extensively by several authors.[6–9] The refractive indices along and across the fiber axis and the optical birefringence are parameters characterizing the molecular orientation and hence physical structure of these materials.

The phenomenon of cold drawing is common to both amorphous and semicrystalline polymers. In the drawing process, the isotropic starting material is transformed into a highly anisotropic fiber structure. The molecular chains are oriented along the drawn direction, and the crystal lamellae are stacked roughly normal to the draw direction.[10]

Orientation in polymers can be produced by several processes, such as hot stretching of a molten polymer followed by rapid cooling of the melt, cold drawing, or cold rolling. The drawing process gives rise to the preferred orientation of the molecular chain axis. The degree of orientation can vary significantly from one fiber to another, depending on the history of the fiber during its manufacture and subsequent processing operations. Orientation in a polymer has been extensively measured by several authors.[11–13]

Statton[14] proposed that shrinkage should be attributed to the refolding of chains that have been pulled out in the drawing process. Crystallinity is generally induced by a high level of strain brought about by stretching and is termed strain- (or stress-) induced crystallization.[15]

A reduction in the entropy (ΔS) due to the stretching process can change the optical properties of polymeric materials. Also, the retractive forces of the network are produced by a decrease in ΔS of freely joined chains when they are stretched.

This work focuses attention on the use of the principal optical parameters obtained by interferometry and mechanical parameters for determining some essential indicative industrial parameters. The mean polarizability of the monomer per unit of volume and other optomechanical parameters were also determined.

THEORETICAL CONSIDERATIONS

The mean values of the refractive indices of the fiber and the total mean birefringence were calculated

Correspondence to: E. A. Seisa (seisa@mans.edu.eg).

with equations extensively used in our previous publications.[16–19] With the Kuhn–Treloar theory, we can calculate the number of chains per unit of volume (ν),[20] which depends on the number of crystallites in the polymer material. For an ideal network[21]

$$\nu = \frac{N_A \rho}{M} \tag{1}$$

where N_A is Avogadro's number, ρ is the polymer density, and M represents the monomer molecular units (molar weight = 162.14) for the viscose fibers. For a collection of chains containing ν chains

$$W = \frac{\nu KT}{2}\left[\left(D^2 - D^{-1}\right) + 3\left(D^{-1} - 1\right)\right] \tag{2}$$

where W is the work per unit of volume, K is Boltzmann's constant, T is the absolute temperature, and D is the draw ratio ($D = l/l_0$, where l_0 is the initial length and l is the elongation produced, and $D = 1 + d$, where d is the strain).

The stress (σ) is related to the elongation as follows:

$$\sigma = \frac{\partial W}{\partial D} = \nu KT\left[D - D^{-2}\right] \tag{3}$$

The elongation leads to a reduction of ΔS:

$$\Delta S = -\frac{1}{2} K\nu\left[(1+d)^2 + \frac{2}{(1+d)} - 3\right] \tag{4}$$

The quantity νKT in eq. (2) is equivalent to the shear modulus (G). This term is sometimes written in terms of the mean molecular mass of the chains (M), that is, between successive points of crosslinkage. Then

$$G = \nu KT = \rho RT/M \tag{5}$$

where R is the gas constant. The shear elastic modulus is related to Young's modulus (E) for elastic materials when Poisson's ratio (μ) is about 0.5, so the elastic tensile modulus is 3 times greater then G.

Calculation of E and μ

The moduli of elasticity (G and E) are related by the following simple equation:

$$E = 3G \tag{6}$$

This defines the relation between E and G to a good approximation for an elastomer.[22]

μ for fibers of a very small radius contracts by loading and, under the assumption of a constant volume, can be obtained as follows:[17]

$$\mu = 1/2D \tag{7}$$

Relations between E, G, and the bulk modulus (B)

By applying and arranging the following equations, we can determine B and the compressibility (β):

$$E = 3B(1 - 2\mu) = 2(1 + \mu)G \tag{8}$$

$$(1 - 2\mu) = E/3 \; B = \beta E/3 \tag{9}$$

Calculation of the cohesive energy density (CED) and square of the solubility parameter (δ)

The value of B was calculated in terms of CED, which represents the energy theoretically required to move a detached segment into the vapor phase. This in turn is related to δ^2:[23]

$$B = 8.04 \text{ (CED)} \tag{10a}$$

$$B = 8.04\delta^2 \tag{10b}$$

The factor 8.04 arises from the Lennard–Jones consideration.

Evaluation of the maximum birefringence (Δn_{max})

The birefringence (Δn) is related to Δn_{max} for fully oriented, so Δn_{max} can be determined with the following relation:[24]

$$\frac{\Delta n}{\Delta n_{max}} = \frac{3}{2}\frac{D^3}{(D^3 - 1)}\left[1 - \frac{1}{\sqrt{(D^3 - 1)}}\sin^{-1}\frac{(D^3 - 1)}{\sqrt{D^3}}\right] - \frac{1}{2} \tag{11}$$

With eq. (11), we evaluated Δn_{max}, and we found that the average value was 0.046 for viscose fibers when it was estimated by the optomechanical method.

Mooney–Rivlin equation

The storable elastic energy of the network (W'') is only a function of the strain invariant. It can be represented by the following equation for uniaxial elongation:

$$W'' = C_1\left[\left(D^2 + 2D^{-1} - 3\right)\right] + C_2\left[D^{-2} + 2D^{-3}\right] \tag{12}$$

where C_1 and C_2 are empirical constants called the Moony Rivlin Coefficients. σ can be calculated with the following equation:[25]

$$\sigma = 2\left[C_1 + C_2 D^{-1}\right]\left[D^2 - D^{-1}\right] \tag{13}$$

Equation (13) is the well-known Mooney–Rivlin equation. A plot of the reduced stress $[\sigma/2(D^2 - D^{-1})]$ as a function of the reciprocal of the elongation (D^{-1}) gives a straight line whose slope is C_2 and whose intercept with the ordinate is C_1. In practice, the constant C_1 has proved to be a useful measure of the crosslink density. The second term can be attributed to energy dissipation resulting from chain interactions during deformation, and in conformity with this view, C_2 becomes zero when the elastomer is swollen by solvents.

Optical stress coefficient (C_s)

The constant C_s is called the optical stress coefficient. The value of this coefficient is dependent on the chemical structure of the polymer. The value of this coefficient also depends solely on the mean refractive index ($\overline{n}$) and the optical anisotropy of the random link, as shown in the following equation:

$$C_s = \frac{2\pi}{45KT}\left[\frac{\left(\overline{n^2}+2\right)^2}{\overline{n}}\right]\left[\alpha^{\|} - \alpha^{\perp}\right] \tag{14}$$

where $\alpha^{\|}$ and $\alpha^{\perp}$ are the polarizabilities along and across the axis of such units, respectively. C_s is independent of the chain length and the degree of crosslinking.

With the previous equation, it can be seen that Δn for elastomers is proportional to the applied stress.

Calculation of the optical configuration parameter ($\Delta\alpha$)

$\Delta\alpha$ is related to C_s as follows:[26]

$$\Delta\alpha = \left(\frac{45KTC_s/2\pi}{\left(\overline{n^2}+2\right)^2}\right)\overline{n} \tag{15}$$

Mean polarizability of the monomer unit ($\overline{\alpha}$)

The refractive index of a polymer depends on the total polarizability of the molecules; this leads to the Lorentz–Lorenz equation with the following equation:[27]

$$\frac{\overline{n^2}-1}{n^2+2} = \frac{\nu\overline{\alpha}}{3\psi} \tag{16}$$

where $\overline{\alpha}$ is caused by the deformation of the electron clouds in and between the molecules of the dielectric under the influence of the effective field (i.e., the internal field) and ψ is the permittivity of free space (8.85×10^{-12} Fm^{-1}).

De Vries[27] reported a theory, based on an internal field with the aid of classical electromagnetic theory, in which he generalized the Lorentz–Lorenz equation. Thus, for monochromatic light, the well-known Lorentz–Lorenz equation becomes the same as eq. (16). The right-hand portion of eq. (16) is proportional to ρ (kg/m^3) of the medium and can also be written as follows:

$$\frac{\overline{n^2}-1}{\overline{n^2}+2} = \overline{\varepsilon}\rho \tag{17}$$

where $\overline{\varepsilon}$ (m^3/kg) is the specific refractivity of the isotropic dielectric.

Δn of the homogeneously uniaxially stretched polymer

With eq. (14), it can be seen that Δn for elastomers is proportional to the applied stress.[21] When the contributions of the chains to the network anisotropy are summed and the Lorentz–Lorenz relation is used to obtain Δn between the refractive indices parallel ($n^{\|}$) and perpendicular ($n^{\perp}$) to the extension direction, the result is

$$n^{\|} - n^{\perp} = \frac{N'\gamma_s}{90\psi}\frac{\left[\overline{n^2}+2\right]^2}{\overline{n}}\left[D^2 - D^{-1}\right] \tag{18}$$

$$C_s = \frac{\gamma_s}{90\psi KT}\frac{\left[\overline{n^2}+2\right]^2}{\overline{n}} \tag{19}$$

where N' is the number of chains between crosslinks per unit of volume at the absolute temperature and γ_s is the segment anisotropy. From eqs. (18) and (19), we can determine γ_s and then N'.

Δn of the partially crystalline polymer

If we assume that the partially crystalline polymer consists of separate crystalline and amorphous parts, the change in the crystal direction on stretching is affine with the deformation of the amorphous matrix, but the crystal does not change in size on stretching. The average orientation angle ($\langle\cos^2\theta_c\rangle$) with respect to the uniaxial stretching extension ratio (D) is

$$\left\langle\cos^2\theta_c\right\rangle = \frac{D^3}{D^3-1}\left[1 - \frac{\tan^{-1}(D^3-1)^{1/2}}{(D^3-1)^{1/2}}\right] \tag{20}$$

If there are M crystals per unit of volume and they have polarizability α_c along the c axis and polarizabilities α_b and α_a ($\alpha_b = \alpha_a$) perpendicular to it, then

Figure 1 Cross section of irregular viscose fibers.

the crystal contribution to Δn of the medium is given by

$$S = \frac{\Delta n}{\Delta \alpha} \frac{18\psi}{\langle P_2(\cos^2 \theta_c)\rangle} \frac{\overline{n}}{[\overline{n^2} + 2]^2} \tag{21}$$

where

$$P_2(\cos^2 \theta_c) = 1/2(3\cos^2 \theta_c - 1) \tag{22}$$

EXPERIMENTAL

Material

The viscose fibers were manufactured by Misr Rayon (Cairo, Egypt). The untreated sample had a glass-transition temperature of 45.9°C. Cross sections of viscose fibers were viewed with a high-power optical microscope and found to be irregular in shape with an area of 1.165×10^{-3} mm^2 (as shown in Fig. 1).

Application of two-beam interferometry

A Pluta microscope was joined to a microstrain device that was designed and discussed in detail previously.[28] This device was modified to measure the stress and strain. The modification enabled us to measure the mechanical properties and correlate them with the optical properties. Viscose fibers were fixed on a microscope slide in a suitable position in the drawing device. A glass coverslip was placed on the viscose fibers, which were immersed in a liquid with a refractive index of 1.528 at 21°C, and monochromatic light with a wavelength of 546.1 nm was used. The device was transferred to the Pluta microscope, which was adjusted for the totally duplicated image of the viscose fibers, in which the two fringes shifted for light vibrating parallel and perpendicularly to the fiber axis. An interference pattern was recorded for each drawing process. Figure 2(a,b) shows two photographs of totally duplicated images for viscose fibers at draw ratios of 1.113 and 1.313.

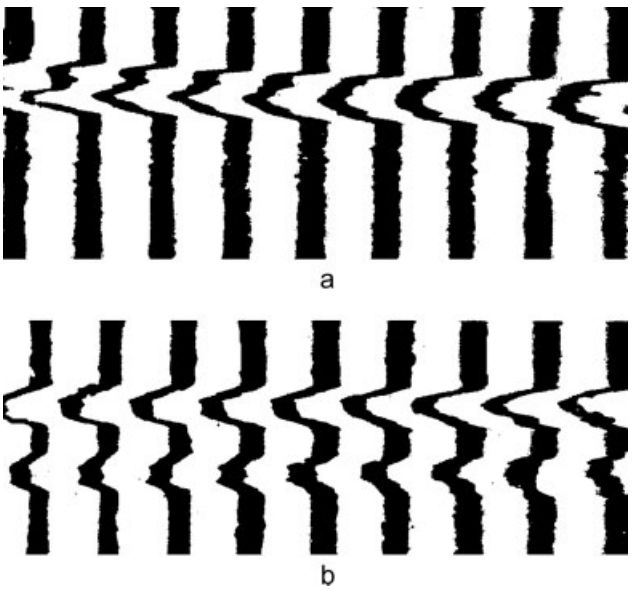

Figure 2 Two-beam interferometry microinterferograms from completely duplicated images of viscose fibers: (a) draw ratio = 1.113 and (b) draw ratio = 1.313.

To estimate the initial draw ratio (D_0) of viscose fibers, the refractive indices and hence Δn were determined with the drawing device. Therefore, plotting Δn as a function of the draw ratio led to a straight line whose equation was in the form of $\Delta n = A + B(D + D_0)$, where D is the experimental draw ratio. For an undrawn fiber ($D = 1$), we considered the fiber medium to be isotropic (i.e., $\Delta n = 0$). Introducing these characteristic values into the linear equation, we obtained the real value of D_0. Also, the extrapolation of Δn versus D should cut the negative part of axis D at D_0. Therefore, the actual draw ratio was found to be $D + 0.113$.[29]

Figure 3 shows the relationship between W and the draw ratios for the viscose fibers, indicating that W increased because of cold drawing. Figure 4 shows the relationship between the reduction of ΔS

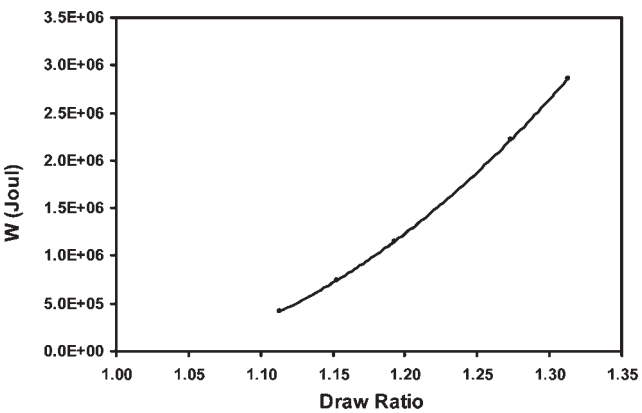

Figure 3 Relation between W and the draw ratio of the viscose fibers.

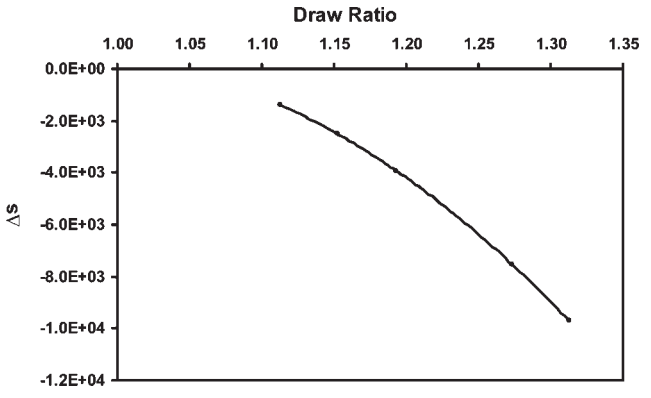

Figure 4 Relation between ΔS and the draw ratio of the viscose fibers.

and the draw ratios. It indicates the decrease in ΔS due to cold drawing, and Figure 5 shows the relationship between Δn and ΔS under different draw ratios, throwing light on the decrease in ΔS and energy changes. Figure 6 describes the relationship between C_s and the draw ratios for the viscose fibers, showing the increase in C_s with different draw ratios, and Figure 7 shows the relationship between $\Delta\alpha$ and the draw ratios. Figure 8 presents the relation between N' and the draw ratios of the viscose fibers; also, Figure 9 shows the relation between the crystals per unit of volume (S) and the draw ratios. Figures 8 and 9 show that N' and S decreased with increasing draw ratios. Table I lists some calculated experimental parameters with different draw ratios: ν, σ, $\varepsilon^{\parallel}$, $\varepsilon^{\perp}$, $\bar{\varepsilon}$, $\bar{\alpha}$, and $\langle\cos^2\theta\rangle$.

Also, Table II lists the values of G, E, μ, B, β, CED, and δ with different draw ratios.

Crystallinity

As is well known, n_{iso}[30] is linearly proportional to the density, and the density shows a linear dependence on the degree of crystallinity (χ_c):[31]

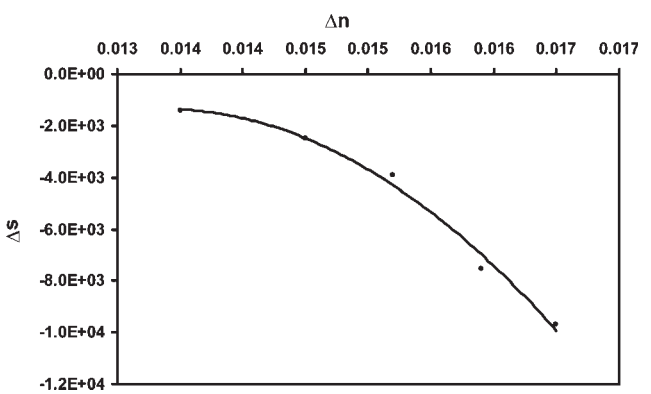

Figure 5 Relation between Δn and ΔS of viscose fibers with different draw ratios.

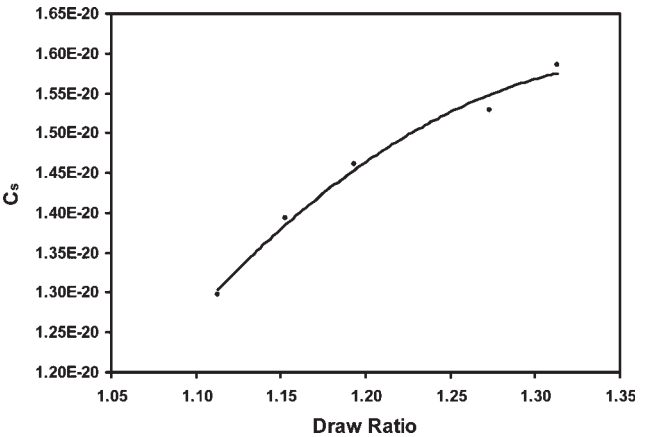

Figure 6 Relation between C_s and the draw ratio of the viscose fibers.

$$\chi_c = [n_{iso} - 1.5077]/0.0456 \quad (23)$$

This equation allows us to evaluate χ_c from n_{iso} at n_{iso} values of 1.5077 (χ_c = 0%) and 1.5533 (χ_c = 100%).

Density equation

The density was determined with the following equation by the well-known crystallinity relation:

$$\rho = \chi_c(\rho_c - \rho_a) + \rho_a \quad (24)$$

where ρ_c is 1.625[32] and ρ_a is 1.489 g/cm^3. Figure 10 shows the variation of the decrease in the density with an increase in the draw ratios of the viscose fibers.

Relation between the true stress (σ_{true}) and strain hardening

If the Gaussian elasticity relation was substituted for the Langevin theory, a true stress–strain curve[33]

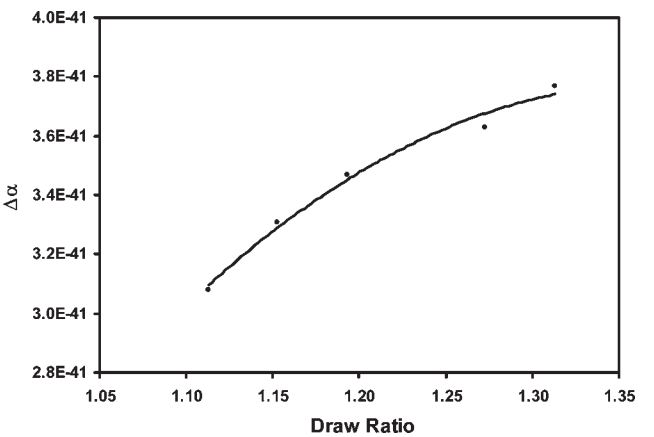

Figure 7 Relation between $\Delta\alpha$ and the draw ratio of the viscose fibers.

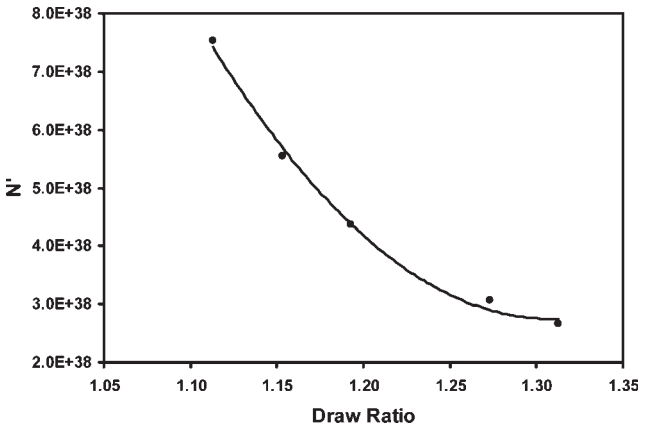

Figure 8 Relation between N' and the draw ratio of the viscose fibers.

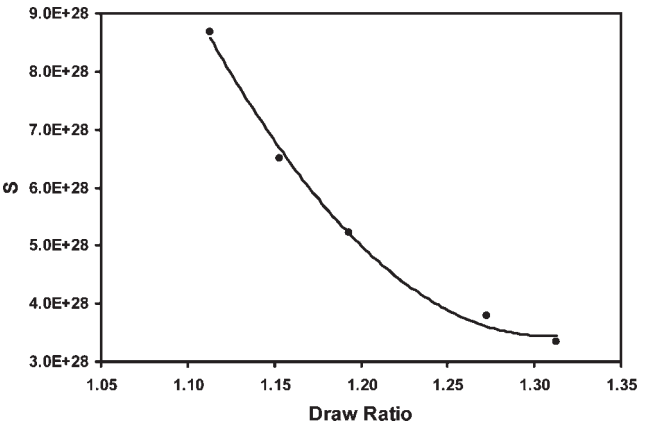

Figure 9 Relation between S and the draw ratio of the viscose fibers.

could be simply represented (Fig. 11) with the following equation:

$$\sigma_{true} = Y + \text{const}(D^2 - 1/D) \tag{25}$$

where σ_{true} is the true stress, that is, the stress which is uniform over the volume of material under consideration; Y is the yield stress; and D is the extension ratio. This equation is subsequently called the Gaussian equation. Equation (25) can also be rearranged to represent the nominal or engineering stress (σ_{eng}):

$$\sigma_{eng} = Y/D + G_p(D - 1/D^2) \tag{26}$$

where G_p is the strain-hardening modulus. Using this form of the equation, we can note that necking conditions require $d\sigma_{eng}/dD$ to be negative at low values of D:

$$d\sigma_{eng}/dD = -Y/D^2 + G_p(1 + 2/D)^2 \tag{27}$$

It should be less than 0 when $D = 1$, for which the critical condition is $Y/G_p > 3$.

RESULTS AND DISCUSSION

Part of the modern trend in fiber research is to alter fiber properties. One of the methods for property modification involves the effects of the cold-drawing process under different conditions. Several studies have been reported on the effects of mechanical processes on the structures of synthetic and natural fibers. The birefringence orientation, density, crystallinity, and elasticity are known as some of the properties that affect the textile quality for the main end use. Thus, the calculated density could also be used to follow the continuous changes occurring during the physical changes of the samples under investigation. The obtained values of the evaluated crystallinity and density were dependent on the nature of the polymer mechanical process.[34–37]

Under cold drawing, results were obtained for the optical and mechanical parameters of a polymeric material that was produced with modified physical properties due to changes in ΔS, W, and W'' and optical parameters. Also, to explain the different variations due to mechanical effects, several interfering structural processes had to be taken into consideration, and they have been discussed in detail elsewhere.[29] Although the degree of orientation always increases in the course of drawing, crystallinity can also change in both directions. Three types of behavior can be distinguished: deformation does not affect the phase structure of an undrawn amorphous sample, it remains amorphous after drawing, and a crystalline sample does not change in its degree of crystallinity; deformation is accompanied by partial destruction of the original structure and a reduction

TABLE I
Values of ν, σ, $\bar{\varepsilon}$, $\varepsilon^{\parallel}$, $\varepsilon^{\perp}$, $\bar{\alpha}$, and $\langle\cos^2\theta\rangle$ with Different Draw Ratios

Draw ratio	ν ($\times 10^{27}$)	σ ($\times 10^6$ Pa)	$\varepsilon^{\parallel}$ ($\times 10^{-4}$ m^3/kg)	$\varepsilon^{\perp}$ ($\times 10^{-4}$ m^3/kg)	$\bar{\varepsilon}$ ($\times 10^{-4}$ m^3/kg)	$\bar{\alpha}$ ($\times 10^{-39}$)	$\langle\cos^2\theta\rangle$
1.113	5.6954	7.083	2.020	1.977	1.998	1.4236	0.3770
1.153	5.6936	9.281	2.022	1.976	1.999	1.4236	0.3918
1.193	5.6917	11.35	2.023	1.975	1.999	1.4237	0.4061
1.273	5.6910	15.18	2.025	1.974	2.000	1.4238	0.4336
1.313	5.6910	16.97	2.026	1.974	2.000	1.4238	0.4468

TABLE II
Values of G, E, μ, B, β, CED, and δ with Different Draw Ratios

Draw ratio	G ($\times 10^7$ Pa)	E ($\times 10^7$ Pa)	μ	B ($\times 10^8$ Pa)	β ($\times 10^{-9}$ Pa^{-1})	CED ($\times 10^7$ Pa^{-1})	δ (Pa)
1.113	2.398	6.950	0.449	2.282	4.383	2.838	5327
1.153	2.4237	6.947	0.434	1.745	5.730	2.171	4659
1.193	2.447	6.945	0.419	1.431	6.988	1.780	4219
1.273	2.493	6.944	0.393	1.079	9.265	1.342	3664
1.313	2.515	6.944	0.381	0.971	10.30	1.208	3475

of the crystallinity; and deformation is accompanied by additional crystallization and an increase in the crystallinity. Figures 4 and 5 show the heat when they were reversibly stretched. These observations were consistent with the view that ΔS of the polymer decreased on stretching. As shown in Figures 8 and 9, N' and S decreased because of deformation from the drawing processes. These decreases were attributed to cold drawing, which may in turn have arisen from changes in ΔS of folded chains of the original structure of the crystalline phase deformation.

From another interpretation perspective, the changes in the obtained results for $\bar{\varepsilon}$, α, C_s, γ_s, and Δn are attributable to modifications of the electrical properties arising from existing space changes and the remaining electric field in the polymers after preparation.

Also, it is important to note that C_s depends only on $\bar{n}$ (which is not in itself a network property) and on the optical anisotropy of the random link. It docs not involve the number of chains per unit of volume and is therefore independent of the degree of crosslinking of the network. Thus, these results for viscose cellulose xanthate show the effect of the molecular structure on strain hardening with a similar cellulose ester.[12]

CONCLUSIONS

From the aforementioned measurements and calculations of the various optical and mechanical parameters and their changes with the cold-drawing process, the following conclusions can be drawn:

1. There are isothermal kinetic changes due to the drawing process that are confirmed by the changes in ΔS, which are accompanied by changes in Δn. Also, the retractive forces of the network are produced by a reduction of ΔS of freely joined chains when they are stretched.
2. Changes in ΔS throw light on the energies that play a role in clarifying the phase boundary between the amorphous and crystalline regions.
3. The application of the Mooney–Rivlin equation shows a nearly linear relationship. The constants C_1 and C_2 were determined to be -4.467×10^4 and 1.1631×10^7, respectively.
4. Δn_{max} (the maximum birefringence observed in the partially (fully) oriented fiber) was achieved with eq. (11), and its average value was equal to 0.046 for viscose fibers; this was an acceptable result according to ref. 27.
5. The mechanical properties Y, G_p, and σ_{eng} change with the applied stress. The mechanical constants of eq. (25), Y and G_p, were found to be 2×10^6 and 2×10^7, respectively.

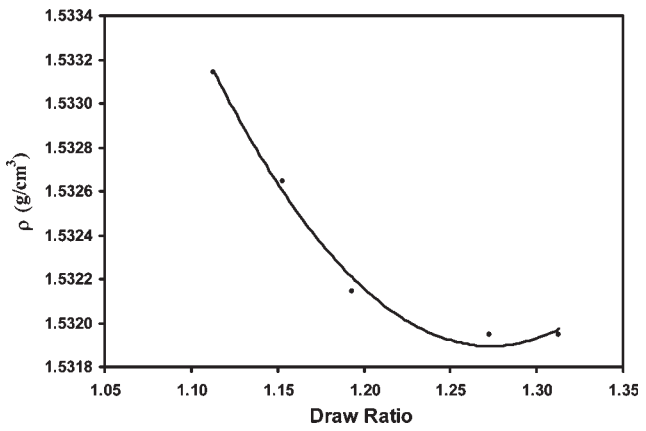

Figure 10 Variation of ρ and the draw ratio of the viscose fibers.

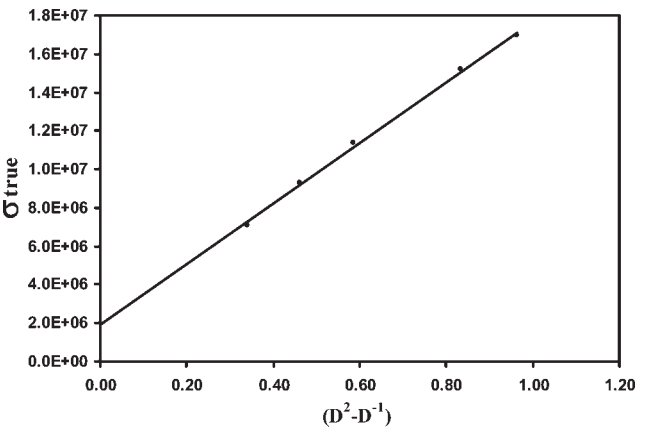

Figure 11 Variation of σ_{true} as a function of $D^2 - 1/D$ of the viscose fibers.

6. Changes in the density are accompanied by changes in the mass redistribution within the fiber chains. This also indicates the changes in the chain (segmental) orientation, which are the result of deformation.

From these results and considerations, we have concluded that the practical importance of these values lies in an acceptable evaluation of optomechanical parameter changes for viscose fibers.

References

1. Mauersberger Mathews, H. R. Textile Fibers, 5th ed.; Wiley: New York, 1947; p 755.
2. Heyn, A. N. Fiber Microscopy; Interscience: London, 1954; p 156.
3. Barakat, N.; Hindelah, A. M. Text Res J 1964, 34, 4357.
4. Fouda, I. M.; Seisa, E. A.; Oraby, A. H. J Appl Polym Sci 1999, 71, 361.
5. Fouda, I. M.; Shabana, H. J Appl Polym Sci 1999, 72, 1185.
6. Barakat, N.; Hamza, A. A. Interferometry of Fibrous Materials; Hilger: Bristol, England, 1990.
7. Fouda, I. M.; Shabana, H. M. J Phys: Condens Matter 1999, 11, 3371.
8. Perena, J. M.; Duckett, R. A. J Appl Polym Sci 1980, 25, 1381.
9. Fouda, I. M.; El-Tonsy, M. M. Polym Plast Technol Eng 2006, 45, 223.
10. Andrew, J. M.; Ward, I. M. J Mater Sci 1970, 5, 411.
11. Hermans, P. H. Contributions to the Physics of Cellulose Fibres; North Holland: Amsterdam, 1949.
12. Ward, I. M. Mechanical Properties of Solid Polymers; Wiley: New York, 1985.
13. Ward, I. M. Structure and Properties of Oriented Polymers; Applied Science: London, 1975; p 57.
14. Statton, W. O. J Polym Sci Part C: Polym Symp 1967, 20, 117.
15. Ward, I. M. Br J Appl Phys 1967, 18, 1165.
16. Fouda, I. M. J Appl Polym Sci 1995, 73, 819.
17. Fouda, I. M. J Appl Polym Sci 2002, 84, 916.
18. Fouda, I. M.; El-Sharkawy, F. M. J Appl Polym Sci 2003, 99, 729.
19. Fonda, I. M.; Kabeel, M. A.; El-Sharkawy, F. M. Polym Polym Compos 1997, 5, 431.
20. Stein, R. S. J Polym Sci 1959, 24, 709.
21. Jenkins, A. D. Materials Science Handbook; North Holland: Amsterdam, 1972; p 505.
22. Sperling, L. H. Introduction to Physical Polymer Science, 2nd ed.; Wiley: New York, 1992; p 161.
23. Vinogradov, G. V.; Ozyura, E. A.; Malikin, A. Y.; Grechano Vaka, V. A. J Polym Sci Part A-2: Polym Phys 1971, 9, 1152.
24. Neil, M. A.; Duckett, R. A.; Ward, I. M. Polymer 1988, 29, 54.
25. Gedde, U. L. F. W. Polymer Physics; Chapman & Hall: London, 1995.
26. Riande, E.; Guzman, J. J Polym Sci Polym Phys Ed 1984, 22, 917.
27. De Vries, H. Colloid Z Polym Sci 1979, 257, 226.
28. Hamza, A. A.; El-Farahaty, K. A.; Helaly, S. A. Opt Appl 1988, 18, 133.
29. Fouda, I. M.; Seisa, E. A. J Appl Polym Sci 2007, 106, 1768.
30. Monobe, S. R.; Kamide, K. Text Plach Sci 1999, 72, 1185.
31. Monobe, S. R.; Iwata, M.; Kamide, K. Polym J 1981, 18, 1.
32. Wunderlich, B. Macromolecular Physics, Crystal Structure, Morphology, Defects; Academic: London, 1973; p 426.
33. (a) Haward, R. N. Polymer 1999, 35, 3858; (b) Ward, I. M. Mechanical Properties of Solid Polymers, 2nd ed.; Wiley: New York, 1985; Chapter 11; (c) Kinloch, A. J.; Young, R. J. The Fracture Behavior of Polymers; Elsevier: London, 1985.
34. Fouda, I. M. Polym Test 1999, 18, 363.
35. Fouda, I. M.; Shabana, H. M. Polym Int 1999, 48, 602.
36. Fouda, I. M.; Shabana, H. M. J Appl Polym Sci 1999, 72, 1185.
37. Fouda, I. M.; Shabana, H. M. Polym Int 1999, 48, 198.